

## Reversible Transformation of Helical Coils and Straight Rods in Cylindrical Assembly of Elliptical Macrocycles

Jung-Keun Kim,<sup>†</sup> Eunji Lee,<sup>†</sup> Min-Cheol Kim,<sup>‡</sup> Eunji Sim,<sup>‡</sup> and Myongsoo Lee<sup>\*†</sup>

Center for Supramolecular Nano-Assembly and Department of Chemistry, Seoul National University, 599 Kwanak-ro, Seoul 151-747, Korea, and Department of Chemistry, Yonsei University, Seoul 120-749, Korea

Received September 3, 2009; E-mail: myongslee@snu.ac.kr

The self-assembly of rigid macrocycles into well-defined nanostructures has been the subject of intense study in recent years, both for basic research and for potential applications.<sup>1</sup> Most rigid aromatic macrocycles self-assemble into cylindrical micelles,<sup>2</sup> while certain macrocycles self-assemble into spherical structures.<sup>3</sup> The main challenge in assembling aromatic building blocks into these nanostructures lies in their capability to respond to external stimuli.<sup>4</sup> To obtain controlled aggregates that are able to respond to external stimuli, however, the more elaborate design of corresponding building blocks is required. Accordingly, we have synthesized amphiphilic aromatic macrocycles with an elliptical shape containing oligoether dendrons that can endow aggregates with a thermo-responsive feature.

We present herein the structural progression in the self-assembly of macrocyclic amphiphiles in water from spheres, helical coils to vesicles with an increase in the molecular length of the elliptical macrocycle, and reversible transformation of the helical coils into straight rods triggered by temperature. The macrocyclic amphiphiles were prepared from the cyclization by a Glaser coupling reaction according to procedures reported previously.<sup>5</sup> The resulting macrocycles characterized by NMR spectroscopy, elemental analysis, and MALDI-TOF mass spectroscopy (Figure S1) were shown to be in full agreement with the structures presented.

The aggregation behavior of the molecules was investigated in aqueous solution by using transmission electron microscopy (TEM). TEM studies showed that all of these macrocyclic amphiphiles self-assemble into stable nanostructures. Figure 2a shows a micrograph obtained from a 0.01 wt % aqueous solution of **1** based on a shorter elliptical macrocycle cast onto a TEM grid. The negatively stained sample with uranyl acetate shows the formation of spherical micelles with a diameter of ~5 nm which is comparable to the molecular length (6.5 nm). This result suggests that the discrete nanostructure consists of an aromatic core in which the rigid macrocycles are stacked on top of each other with mutual rotation and an oligoether dendron exterior that is exposed to a water environment.

Interestingly, molecule **2** based on an intermediate length of elliptical macrocycle self-assembles into helical coils. The evidence for the formation of the nonspherical structure in aqueous solution was also provided by cryo-TEM experiments performed with 0.01 wt % solution (Figures 2b, S3). Examination of a large area TEM image shows helical coils to be the predominant species in solution. Closer examination of the image reveals that the cylindrical micelles with a cross-sectional diameter of ~3 nm are curved to form helical coils with a uniform diameter of ~30 nm and a regular pitch of ~10 nm (Figure 2c). The aromatic cores appear to be dark, whereas the solvated oligoether dendrons are not directly visible.<sup>6</sup> Thus, comparison with the estimated length of the macrocycle of 2.8 nm

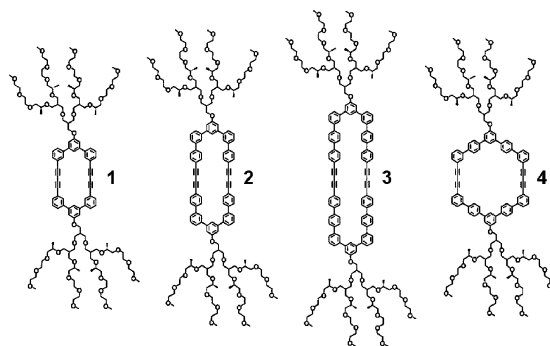


Figure 1. Chemical structure of amphiphilic rigid macrocycles 1–4.

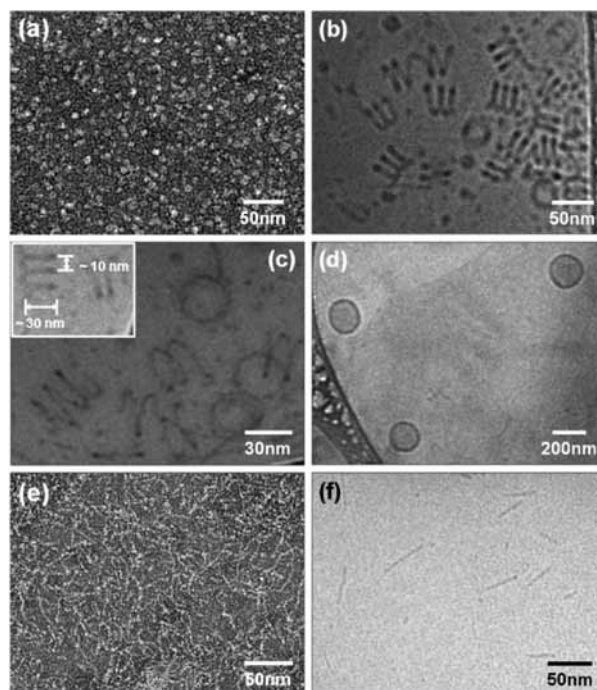
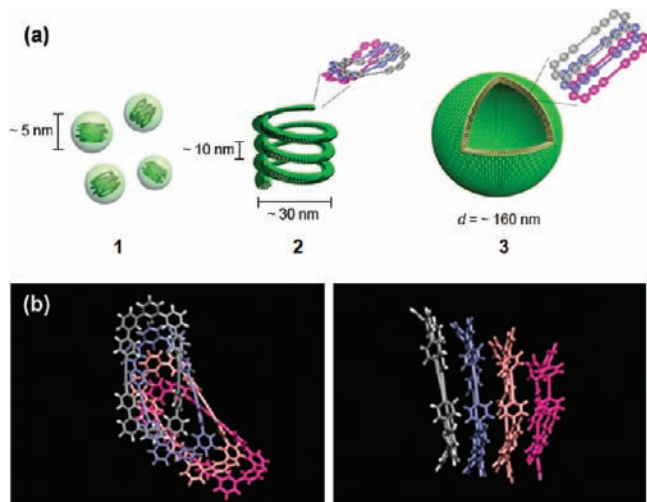


Figure 2. (a) TEM image of spherical micelles formed from **1**. (b,c) Cryo-TEM images of helical coils formed from **2**. (d) Cryo-TEM image of vesicles formed from **3**. (e) TEM and (f) cryo-TEM images of cylindrical micelles formed from **4**.

suggests that the macrocycle stacks on top of each other with mutual rotation surrounded by oligoether dendrons. The solution displays a significant Cotton effect in the aromatic unit, indicating the presence of one-handed helical aggregates. This is in sharp contrast to the solution behavior of **1** and **3** which shows a complete lack of a Cotton effect (Figure S4).

<sup>†</sup> Seoul National University.

<sup>\*</sup> Yonsei University.



**Figure 3.** (a) Schematic representation of the self-assembled structures of 1–3. (b) Simulated structures of the macrocycle molecule 2. Each molecule is colored differently for clarity. Top view (left) and side view (right).

An aqueous solution of 3 based on an elongated macrocycle with a higher aspect ratio is characterized by the presence of vesicular aggregates. When the aqueous solution (0.01 wt %) is allowed to be stabilized and then cast onto a TEM grid, the image stained with uranyl acetate reveals spherical objects with diameters ranging from several tens to few hundreds of nanometers. DLS studies (Figure S2) revealed that the spherical object has an average diameter of  $\sim 160$  nm, which is in good agreement with the size observed by TEM (Figure S5). A cryo-TEM image confirms the presence of spherical aggregates with a dark outer circle expected from the 2D projection of vesicular structures with a uniform thickness of  $\sim 4$  nm. Considering the calculated length of the macrocycle is 3.7 nm, the rigid macrocycle packs into a monolayer structure with the polar oligoether dendritic side chains exposed to water (Figure 2d).

On the basis of the results described above, the possible models responsible for the generation of the self-assembled structures depending on the length of the aromatic core can be presented as shown in Figure 3a. As the molecular length of the elliptical aromatic unit is increased, structural transformation takes place from sphere to helical coils to monolayered vesicles, in the order of decreasing interfacial curvature. This structural progression is most probably due to increasing  $\pi$ - $\pi$  stacking and hydrophobic interactions. Qualitatively, the structural change with the variation in the molecular length of aromatic units resembles that reported for other amphiphilic systems.<sup>7,8</sup> Compared to reported intermediate cylindrical structures, however, a unique feature of our systems is that the cylindrical micelles are curved in a regular way to form well-defined helical coils.

To gain insight into the origin of the self-assembly into helical coils, *ab initio* simulations were performed using the Gaussian 03 package.<sup>9</sup> Using various conformations of a single molecule including a stable boat conformation, we optimized the structure by increasing the number of molecules until four molecules are stacked. Relative energies of stacked structures indicate that the helical secondary structure becomes stabilized as more molecules are assembled (Table S1). As the molecules stacked on top of each other, the molecule with a boat conformation is somewhat slipped and staggered with respect to its neighbors to reduce steric hindrance between the nonplanar macrocycles (Figure 3b). The slipped stacking was also confirmed experimentally by UV-vis spectra,

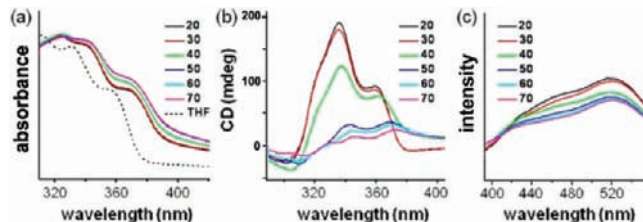


**Figure 4.** (a) UV-vis absorption, (b) circular dichroism and (c) fluorescence spectra of 2 in aqueous solution (0.01 wt %), with temperature variation ( $^{\circ}\text{C}$ ).

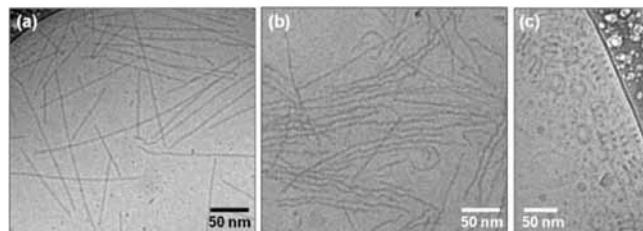


**Figure 5.** Cryo-TEM images of (a) straight rods at 50  $^{\circ}\text{C}$ ; (b) undulated rods on cooling to room temperature, then 6 h annealing; and (c) helical coils after 3 days annealing of 2 in aqueous solution (0.01 wt %).

in which an absorption band maximum at 323 nm in THF solution was shown to be red-shifted by 20 nm in aqueous solution (Figure 4a).<sup>10</sup>

To investigate the role of the elliptical shape of the macrocycle for the helical coil structure, we have modified the macrocycle from elliptical to more circular in shape to form an analogue (4) to molecule 2 with the aim of interference of anisotropic interactions along the stacking axis. Since the dendritic building blocks are based on being identical, the shape of the aggregates may mainly be attributed to the variation in the aspect ratio of the elliptical macrocycle. As shown in Figure 2e–f, 4 self-assembles into cylindrical micelles without any regular curvature with a diameter of  $\sim 6$  nm, indicating that the rigid macrocycles are stacked on top of each other with mutual rotation along the stacking axis. This result implies that the formation of helical coils originates from the unique slipped stacking arrangement of the elliptical macrocycles with a high aspect ratio.

Remarkably, the self-assembled helical coils undergo a reversible phase transition at 40  $^{\circ}\text{C}$ . Upon heating to 50  $^{\circ}\text{C}$ , cryo-TEM of the solution revealed straight rod-like micelles with a uniform diameter of  $\sim 3$  nm and lengths of several hundreds of nanometers (Figures 5a, S9). This result indicates that the helical coils spontaneously unfold into straight rods without any noticeable changes in cross-sectional diameter. On cooling to room temperature, the straight rods started to be undulated (Figure 5b). Complete recovery to the original helical coils was observed over a period of 3 days of resting (Figure 5c). This indicates that the structural transformation between helical coils and straight rods are accompanied by considerable hysteresis. This was further confirmed by CD measurements with annealing times at room temperature (Figure S10). On heating, the phase transition leads to a fast spectral change. However, complete recovery to the original CD profile requires 3 days. This hysteretic behavior in the coiling motion of the straight rods seems to arise from the strong kinetic effect related to the slow breakup of  $\pi$ - $\pi$  stacking interactions between the rigid macrocycles when the straight rods are coiled.

This transition can be explained by considering the lower critical solution temperature (LCST) behavior of the dendritic ethylene oxide chains in aqueous media.<sup>11</sup> The LCST temperature was



**Figure 6.** Schematic representation of reversible transformation of helical coils and straight rods of elliptical macrocycles.

subsequently determined to be 40 °C by turbidity measurements. (Figure S8). At room temperature, the ethylene oxide chains are fully hydrated and thus adopt a random coil conformation. Above the LCST, they are dehydrated to be hydrophobic. As a result, the aromatic cycles are more closely packed due to enhanced hydrophobic environments. This packing consideration is reflected in the increased extent of fluorescence quenching upon heating (Figure 4c).<sup>12</sup> The strengthened  $\pi$ - $\pi$  interactions would lead to a more planar conformation of the elliptical macrocycles. This is supported by temperature-dependent UV-vis (Figure 4a) and CD measurements (Figure 4b). Upon heating to the LCST, an absorption maximum is red-shifted by  $\sim 10$  nm and the shape of the CD spectrum changes, indicating the transformation into a different helical structure through a molecular reorganization within the cylindrical superstructure.<sup>13</sup> The bathochromic shift in both an absorption maximum in UV-vis and a zero crossing point in CD may be attributed to the transformation of a conformer with more conjugation within the macrocycle.<sup>14</sup> Consequently, the closely packed macrocycles with a more flat conformation are staggered with respect to each other with a one-handedness along the stacking axis to form helical rods (Figure 6). Therefore, it can be considered that the structural transformation from helical coils to straight rods is accompanied by the conformational change of the boat-shaped macrocycle into a more planar conformation.

In summary, we have demonstrated that, as the molecular length of an elliptical macrocycle is increased, the self-assembled structure changes from spherical micelles to helical coils and finally to monolayered vesicles, in the order of decreasing interfacial curvature. The most notable feature of the elliptical macrocycles investigated here is their ability to self-assemble into helical coils. More importantly, the helical coils reversibly transform into straight rods upon heating while maintaining the supramolecular chirality. This structural transition is accompanied by conformational change of the elliptical macrocycles from a boat conformation to a more planar conformation. The thermoresponsive feature of the helical fibers represents a significant contrast to other dynamic helical fibers which show a simple extension-contraction motion or unfold into random coils with loss of supramolecular chirality.<sup>15</sup> Such cylindrical aggregates with dynamic structural changes may provide a new strategy for creating intelligent nanomaterials with internal channels.

**Acknowledgment.** This work was supported by the National Creative Research Initiative Program of the Korean Ministry of

Science and Technology and was partially funded by U.S. Air Force (Air Force Office of Scientific Research) under Grant FA2386-09-1-4116. E.S. acknowledges the KOSEF grant funded by the Korea government (MEST) (No. 2009-0054064). J.K.K., E.L., and M.C.K. acknowledge a fellowship of the BK21 program.

**Supporting Information Available:** Detailed synthetic procedures, <sup>1</sup>H NMR and <sup>13</sup>C NMR data. This material is available free of charge via the Internet at <http://pubs.acs.org>.

## References

- (a) Zhang, W.; Moore, J. S. *Angew. Chem., Int. Ed.* **2006**, *45*, 4416–4439. (b) Höger, S. *Chem.—Eur. J.* **2004**, *10*, 1320–1329. (c) Zhao, D.; Moore, J. S. *Chem. Commun.* **2003**, 807–818. (d) Yamaguchi, Y.; Yoshida, Z.-i. *Chem.—Eur. J.* **2003**, *9*, 5430–5440. (e) Chan, J. M. W.; Tischler, J. R.; Kooi, S. E.; Bulović, V.; Swager, T. M. *J. Am. Chem. Soc.* **2009**, *131*, 5659–5666. (f) Grave, C.; Schlüter, A. D. *Eur. J. Org. Chem.* **2002**, 3075–3098.
- (a) Balakrishnan, K.; Datar, A.; Zhang, W.; Yang, X.; Naddo, T.; Huang, J.; Zuo, J.; Yen, M.; Moore, J. S.; Zang, L. *J. Am. Chem. Soc.* **2006**, *128*, 6576–6577. (b) Rosselli, S.; Ramminger, A.-D.; Wagner, T.; Lieser, G.; Höger, S. *Chem.—Eur. J.* **2003**, *9*, 3481–3491. (c) Rosselli, S.; Ramminger, A.-D.; Wagner, T.; Siliu, B.; Wiegand, S.; Häußler, W.; Lieser, G.; Scheumann, V.; Höger, S. *Angew. Chem., Int. Ed.* **2001**, *40*, 3137–3141. (d) Gallant, A. J.; MacLachlan, M. J. *Angew. Chem., Int. Ed.* **2003**, *42*, 5307–5310. (e) Ryu, J.-H.; Oh, N.-K.; Lee, M. *Chem. Commun.* **2005**, 1770–1772.
- (a) Seo, S. H.; Chang, J. Y.; Tew, G. N. *Angew. Chem., Int. Ed.* **2006**, *45*, 7526–7530. (b) Wang, D.; Hsu, J. F.; Bagui, M.; Dusevich, V.; Wang, Y.; Liu, Y.; Holder, A. J.; Peng, Z. *Tetrahedron Lett.* **2009**, *50*, 2147–2149.
- (a) Snir, Y.; Kamien, R. D. *Science* **2005**, *307*, 1067. (b) Lee, C. C.; Grenier, C.; Meijer, E. W.; Schenning, A. P. H. J. *Chem. Soc. Rev.* **2009**, *38*, 671–683. (c) Ajayaghosh, A.; Praveen, V. K. *Acc. Chem. Res.* **2007**, *40*, 644–656.
- (a) Liu, W.-J.; Zhou, Y.; Zhou, Q.-F.; Ma, Y.; Pei, J. *Org. Lett.* **2008**, *10*, 2123–2126. (b) Höger, S.; Enkelmann, V. *Angew. Chem., Int. Ed.* **1995**, *34*, 2713–2716. (c) Tobe, Y.; Utsumi, N.; Kawabata, K.; Naemura, K. *Tetrahedron Lett.* **1996**, *37*, 9325–9328.
- (a) Zheng, Y.; Won, Y.-Y.; Bates, F. S.; Davis, H. T.; Scriven, L. E.; Talmon, Y. *J. Phys. Chem. B* **1999**, *103*, 10331–10334. (b) Li, Z.; Kesselman, E.; Talmon, Y.; Hillmyer, M. A.; Lodge, T. P. *Science* **2004**, *306*, 98–101. (c) Lee, E.; Jeong, Y.-H.; Kim, J.-K.; Lee, M. *Macromolecules* **2007**, *40*, 8355–8360.
- (a) Kim, B.-S.; Hong, D.-J.; Bae, J.; Lee, M. *J. Am. Chem. Soc.* **2005**, *127*, 16333–16337. (b) Kim, J.-K.; Lee, E.; Huang, Z.; Lee, M. *J. Am. Chem. Soc.* **2006**, *128*, 14022–14023.
- (a) Zupancich, J. A.; Bates, F. S.; Hillmyer, M. A. *Macromolecules* **2006**, *39*, 4286–4288. (b) Danino, D.; Talmon, Y.; Zana, R. *Langmuir* **1995**, *11*, 1448–1456.
- See Supporting Information.
- (a) Harrison, W. J.; Mateer, D. L.; Tiddy, G. J. T. *J. Phys. Chem.* **1996**, *100*, 2310–2321. (b) Adachi, K.; Chayama, K.; Watarai, H. *Langmuir* **2006**, *22*, 1630–1639. (c) Würthner, F. *Chem. Commun.* **2004**, 1564–1579.
- (a) Dormidontova, E. E. *Macromolecules* **2002**, *35*, 987–1001. (b) Kim, J.-K.; Lee, E.; Lim, Y.-b.; Lee, M. *Angew. Chem., Int. Ed.* **2008**, *47*, 4662–4666.
- Moon, K.-S.; Kim, H.-J.; Lee, E.; Lee, M. *Angew. Chem., Int. Ed.* **2007**, *46*, 6807–6810.
- George, S. J.; Ajayaghosh, A.; Jonkheijm, P.; Schenning, A. P. H. J.; Meijer, E. W. *Angew. Chem., Int. Ed.* **2004**, *43*, 3422–3425.
- Chen, Z.; Baumeister, U.; Tschierske, C.; Würthner, F. *Chem.—Eur. J.* **2007**, *13*, 450–465.
- (a) Kim, H.-J.; Lee, E.; Park, H.-s.; Lee, M. *J. Am. Chem. Soc.* **2007**, *129*, 10994–10995. (b) Kim, H.-J.; Lim, Y.-b.; Lee, M. *J. Polym. Sci., Part A* **2008**, *46*, 1925–1935. (c) Yashima, E.; Maeda, K.; Sato, O. *J. Am. Chem. Soc.* **2001**, *123*, 8159–8160. (d) Prince, R. B.; Saven, J. G.; Wolynes, P. G.; Moore, J. S. *J. Am. Chem. Soc.* **1999**, *121*, 3114–3121. (e) Zhong, S.; Cui, H.; Chen, Z.; Wooley, K. L.; Pochan, D. J. *Soft Matter* **2008**, *4*, 90–93.

JA907462H